

Approximate Burst Strength of Thin-Walled Cylinders with Hemispherical Caps

N. A. WEIL,* M. A. SALMON,† AND C. J. COSTANTINO‡
IIT Research Institute, Chicago, Ill.

An approximate solution is presented for the bursting strength of thin-walled cylinders with hemispherically capped ends. Deformation theory of plasticity is used, together with the Mises yield criterion and its associated flow rule. Solutions are presented for materials that strain-harden according to a Ludwik power law relationship. Results obtained are compared with those for cylinders with rigid ends to determine the influence of end restraint on burst pressure. Numerical results are presented for cylinder lengths varying from zero (sphere) to infinity and for a range of hardening coefficients from 0 to 1.0. For cylinders with a length/diameter ratio l larger than 2, the effect of end restraint, as represented by spherical heads or rigid caps, upon the burst strength is small, amounting to less than 13%. However, for values of $l < 2.0$, this effect becomes significant, the rigidly capped cylinder being considerably stronger than the hemispherically headed one. Furthermore, both shells are considerably stronger than the infinitely long cylinder.

Nomenclature

L	= half-length
l	= L/r_0 , dimensionless length parameter
n	= hardening exponent for parabolic strain-hardening law
p	= internal pressure, psi
α	= $pr_0/\sigma_0 t_0$, dimensionless pressure ratio
R	= radius of curvature of cylinder generator, in.
\bar{R}	= R/r_0 , dimensionless radius of curvature
r	= circumferential radius, in.
r_0	= original circumferential radius, in.
r_c	= radius of hemispherical cap, in.
ρ	= r/r_0 , dimensionless circumferential radius
ρ_c	= r_c/r_0 , dimensionless end radius of caps
t	= shell thickness, in.
t_0	= original shell thickness, in.
η	= t/t_0 , dimensionless thickness
ϵ	= effective strain
$\epsilon_r, \epsilon_\phi, \epsilon_\theta$	= true strain in thickness, meridional and circumferential directions
θ, ϕ	= circumferential and meridional angle
σ	= effective stress, psi
σ_0	= strength measure for strain-hardening material, psi
$\sigma_\phi, \sigma_\theta$	= membrane stresses, psi
$\bar{\sigma}$	= σ/σ_0 , dimensionless stress
β	= $\sigma_\phi/\sigma_\theta$, ratio of stresses at crown of cylinder

Subscripts and superscripts

*	= functional values at instability (bursting)
1	= quantities at the crown (midlength) of the cylinder
'	= differentiation with respect to ρ_1

I. Introduction

BECAUSE of current interest in reactor-containment vessels and rocket motor or missile cases, a need has developed to refine and improve methods of design and analysis of thin-walled vessels. One of the major problems in this area is the determination of the effect of finite length or the

nature of the end closure on the bursting strength of thin cylindrical shells.

The solution of the problem of the deformation of plastic membrane shells of revolution under internal pressure is complicated by the fact that, except for spheres and infinite cylindrical shells, the ratio of the membrane stresses at a material point changes as the membrane deforms. An exact solution requires that during deformation the strain increments be related to the stresses and stress increments by the flow law appropriate to the yield condition. Thus, in general, it is necessary to follow the deformation from the initial to the final state in a step-by-step procedure to get an exact solution. It has been found possible to avoid this general requirement in the case of cylindrical membranes with rigid end closures for a linear strain-hardening material obeying the Tresca yield condition, and load-deformation curves have been obtained for a range of length-diameter ratios with several values of the hardening constant.¹

In the deformation theory of plasticity, the assumption is made that the plastic strains are determined uniquely by the current state of stress and do not depend on the entire load history. The predictions of this theory often have been in good agreement with experimental results; the theory of the bulge test is a good example,² and in any event deformation theory offers the only practicable method of obtaining solutions in many cases.

A method has been developed³ for obtaining deformation theory solutions for the cylindrical membrane with rigid end closures using the Tresca yield condition in conjunction with the flow rule appropriate to the von Mises yield condition. A material with a stress strain relation of the form $\sigma = \sigma_0 \epsilon^n$ is assumed. The method requires numerical integration to obtain solutions, and numerical results are given for a single case. The method has been extended to apply to cylinders with rigid caps under loads varying in the axial direction,⁴ with numerical results again given for a specific problem. This method also has been applied to develop the system of nonlinear differential equations for the general case of axisymmetric shell under an axially varying internal pressure, but no numerical results are given.⁴

The present paper presents the results of an approximate method of solution of the problem of the pressurized membrane with hemispherical end caps. The basis for the solution is the assumption that the deformed shell has the shape shown in Fig. 1b. The shell profile is made up of two tangent circular arcs of radius of R and r_c . In order to fix these geometric quantities as well as the value of the internal pres-

Received by IAS November 16, 1962; revision received June 12, 1963. The work reported here was done by the authors at Armour Research Foundation of Illinois Institute of Technology for the U. S. Atomic Energy Commission under Contract No. AT(11-1)-528, "Studies of Reactor Containment." Permission to publish the results is acknowledged gratefully.

* Now Vice President, Research and Development, Cummins Engine Corporation.

† Senior Scientist, Mechanics Research Division.

‡ Research Engineer, Mechanics Research Division.

sure, it also is required that the von Mises yield condition and the associated integrated flow law be satisfied at points *A* and *C* on the profile. Thus, the solutions satisfy the requirements of deformation theory at these two points, whereas an exact solution would meet the requirements at every point. The accuracy of the results given by this approximate method depends on how well the assumed profile approximates the actual deformed shape, and how sensitive the results are to changes in the form of the assumed profile. It was found in developing a similar method of solution for the cylinder with rigid end caps⁵ that the results were relatively insensitive to variations in the assumed form of the profile (sine curve, parabola, circular arc), so that the proposed method appears to present a plausible approach to obtaining approximate solutions to an unsolved problem.

II. Basic Equations

Equilibrium Equations

Since at the pole of the end cap (point *C* in Fig. 1b) the shell is locally spherical, the meridional and circumferential stresses, σ_ϕ and σ_θ , are equal and are related to the pressure *p* by the formula

$$\sigma_\phi = \sigma_\theta = pr_e/2t \quad (1)$$

For equilibrium at point *A*, the crown of the cylinder, one has

$$\sigma_\phi = pr_1/2t_1 \quad (2)$$

and

$$(\sigma_\phi/R) + (\sigma_\theta/r_1) = p/t_1 \quad (3)$$

Combining these equations gives

$$\beta = \sigma_\phi/\sigma_\theta = R/(2R - r_1) \quad (4)$$

for the ratio of the principal stresses at the crown.

Plastic Stress-Strain Relations

In the present problem the principal stress in the direction normal to the shell is relatively small and may be assumed to be zero. Von Mises yield condition for a state of plane stress in terms of the principal stresses σ_θ and σ_ϕ is

$$(\sigma_\phi^2 - \sigma_\phi\sigma_\theta + \sigma_\theta^2)^{1/2} = \sigma \quad (5)$$

where σ is the current yield stress in simple tension; it is assumed that the material follows the Ludwik law of strain-hardening:

$$\sigma = \sigma_0\epsilon^n \quad (6)$$

It has been shown⁶ that under the assumptions of deformation theory the current yield stress for a material subjected to biaxial loading is obtained by using the value of the effective strain

$$\epsilon = (2/3)^{1/2}(\epsilon_\phi^2 + \epsilon_\phi\epsilon_\theta + \epsilon_\theta^2)^{1/2} \quad (7)$$

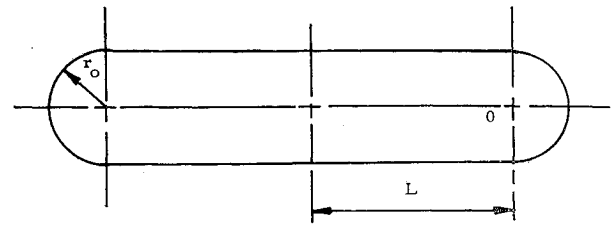
in the tensile test stress-strain relation [Eq. (6)]. It also is shown that the plastic stresses and strains are related by the flow law:

$$\epsilon_\theta/\epsilon_\phi = (2\sigma_\theta - \sigma_\phi)/(2\sigma_\phi - \sigma_\theta) \quad (8)$$

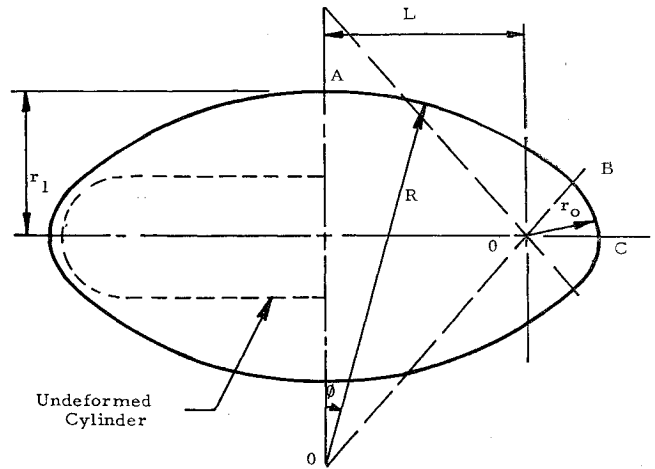
The system of Eqs. (5-8) is sufficient to determine the values of σ_ϕ , σ_θ , ϵ_ϕ , and ϵ_θ if any two of these quantities are given. The third principal strain, the thickness strain ϵ_r , then can be determined from the equation

$$\epsilon_r + \epsilon_\phi + \epsilon_\theta = 0 \quad (9)$$

which expresses the condition that plastic strains produce no volume change.



a) Undeformed Cylinder



b) Deformed Cylinder

Fig. 1 Assumed circular profile of deformed cylinders with hemispherical caps.

Strain Displacement Relations

At the pole of the end cap, the true strains are

$$\epsilon_\phi = \epsilon_\theta = \log(r_e/r_0) = \log \rho_e \quad (10)$$

Using Eq. (10) in Eq. (9) gives

$$\epsilon_r = \log(t/t_0) = \log \eta = -2\log \rho_e \quad (11)$$

At the crown of the cylinder, the true circumferential strain is

$$\epsilon_\theta = \log(r_1/r_0) = \log \rho_1 \quad (12)$$

III. Derivation of the Pressure-Deformation Relations

The assumption that the profile of the deformed shell is made up of tangent circular arcs as shown in Fig. 1b gives the geometrical relation between the radii *R* and *r_e*:

$$R = (L^2 + r_1^2 - r_e^2)/[2(r_1 - r_e)] \quad (13)$$

If *r₁* is specified and *r_e* is assumed to be known, Eq. (13) fixes the value of *R*. The stress ratio β at the crown of the cylinder then is given by Eq. (4). The values of β and ϵ_θ [given by Eq. (12)] are then sufficient to determine σ_θ , σ_ϕ , and ϵ_ϕ from Eqs. (5-8). Finally, the values of the thickness and meridional stress along with the value of *r₁* are substituted into Eq. (2) and the resulting equation solved for the unknown pressure *p*. The formulas obtained with this procedure are, omitting some intermediate calculations,

$$\beta = \frac{L^2 + r_1^2 - r_e^2}{2(L^2 - r_1\rho_e + r_e^2)} \quad (14)$$

$$\epsilon_\phi = \frac{2\beta - 1}{2 - \beta} \log \rho_1 \quad (15)$$

$$\epsilon = \frac{2}{(2 - \beta)} (1 - \beta + \beta^2)^{1/2} \log \rho_1 \quad (16)$$

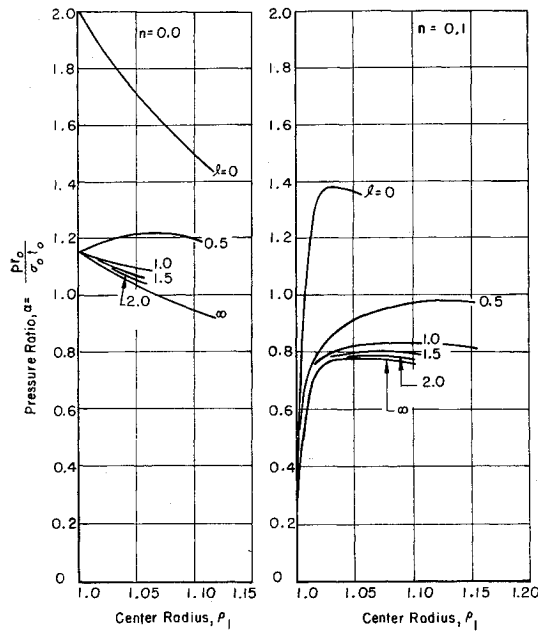


Fig. 2 Pressure-center radius curves for cylinders with hemispherical caps, $n = 0.0$ and 0.1 .

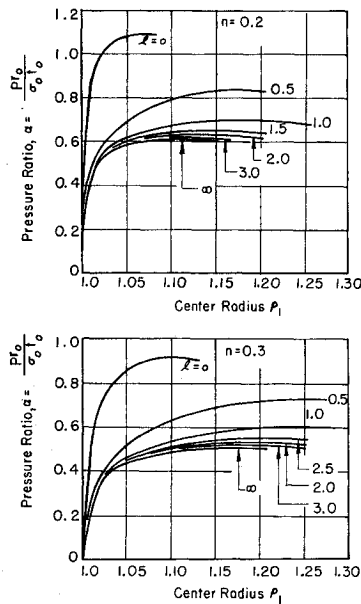


Fig. 3 Pressure-center radius relations for cylinders with hemispherical caps, $n = 0.2$ and 0.3 .

$$\sigma_\phi = \beta(1 - \beta + \beta^2)^{-1/2} \sigma \quad (17)$$

$$\sigma_\phi = \sigma_0 \beta \left(\frac{2}{2 - \beta} \right)^n (1 - \beta + \beta^2)^{(n-1)/2} \log^n \rho_1 \quad (18)$$

$$\epsilon_r = \log \eta = - \frac{(1 + \beta)}{(2 - \beta)} \log \rho_1 \quad (19)$$

$$p = 2\sigma_\phi t_1 / r_1 \quad (20)$$

$$\alpha = \frac{p r_0}{\sigma_0 t_1} = 2\rho_1^{[3/(\beta-2)]} \beta(1 - \beta + \beta^2)^{(n-1)/2} \times \left(\frac{2}{2 - \beta} \right)^n \log^n \rho_1 \quad (21)$$

Equation (21) with the value of β given by Eq. (14) specifies the pressure-deformation relation for a given cylinder as a function of ρ_e , the radius of the end caps. The value of ρ_e is fixed by the requirement that the equilibrium condition

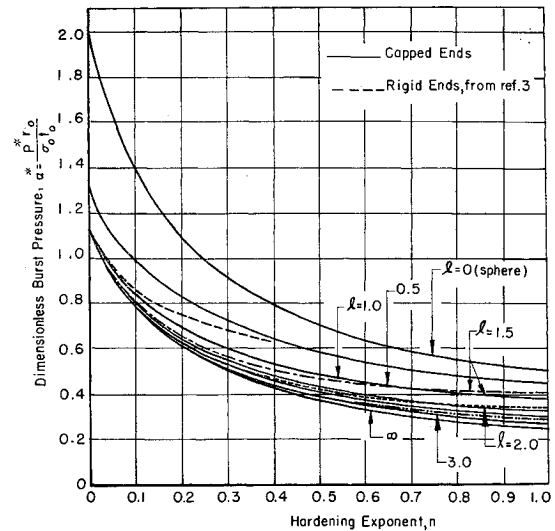


Fig. 4 Influence of end restraint on burst pressure.

[Eq. (1)], the stress-strain relations [Eqs. (5-8)], and the strain-displacement relations [Eqs. (10-11)] be satisfied at the pole of the end cap. This gives a second equation for the pressure ratio as a function of ρ_e :

$$\alpha = (2^{n+1}/\rho_e^3) \log^n \rho_e \quad (22)$$

The pressure-center radius relationship is given by the system of Eqs. (21, 22, and 14). In the case $n = 0$, the material does not harden but is rigid/perfectly plastic with a yield stress equal to σ_0 . For a material of this type, yielding of the cylindrical portion starts when the circumferential stress reaches the value σ_0 , whereas the stress in the cap equals $\sigma_0/2$. The pressure may increase with increasing deformation if the shell is short, but it cannot increase to the point where yielding at the pole of the end cap begins. This follows from the fact that a spherical shell of perfectly plastic material decreases in strength as its radius increases (the burst pressure is the pressure required to initiate yielding), but a capped cylinder must always have a lower burst strength than the corresponding sphere. Therefore, in the case $n = 0$, $\rho_e = 1$, and Eqs. (14) and (21) reduce to

$$\beta = \frac{l^2 + \rho_1^2 - 1}{2(l^2 - \rho_1 + 1)} \quad (23)$$

$$\alpha = 2\rho_1^{[3/(\beta-2)]} \beta(1 - \beta + \beta^2)^{-1/2} \quad (24)$$

Typical pressure-displacement curves for cylinders of various lengths are shown in Figs. 2 and 3. The curves for $l = 0$ and $l = \infty$ represent the limiting cases of the sphere and infinite cylinder. The analysis for these cases is given in Ref. 7. The pressure-radius relations for these two cases also can be obtained from Eq. (21) by substitution of the appropriate value of β :

Sphere ($\beta = 1$, $\rho = \text{radius}$)

$$\alpha = (2^{n+1}/\rho^3) \log^n \rho \quad (25)$$

Infinite Cylinder ($\beta = \frac{1}{2}$, $\rho = \text{radius}$)

$$\alpha = (2/3^{1/2})^{n+1} (1/\rho^2) \log^n \rho \quad (26)$$

IV. Instability Condition

If the value of β from Eq. (14) is substituted into Eq. (21), the resulting equation for the pressure is of the form

$$\alpha = f_1[\rho_1, \rho_e(\alpha)] \quad (27)$$

The functional relationship between α and ρ_e given in Eq. (22) may be written as

$$\alpha = f_2(\rho_e)$$

The total derivative of α with respect to ρ_1 is

$$\frac{d\alpha}{d\rho_1} = \frac{\partial f_1}{\partial \rho_1} + \frac{\partial f_1}{\partial \rho_e} \frac{d\rho_e}{d\alpha} \frac{d\alpha}{d\rho_1}$$

where

$$d\alpha/d\rho_e = df_2/d\rho_e$$

Solving for $d\alpha/d\rho_1$ gives the result

$$\frac{d\alpha}{d\rho_1} = \frac{f_1'}{1 - [(\partial f_1/\partial \rho_e)/(\partial f_2/\partial \rho_e)]} \quad (28)$$

where $f_1' = \partial f_1/\partial \rho_1$ is obtained by differentiation of Eq. (21) as

$$f_1' = \alpha \left\{ \beta' \left[\frac{2 - \beta}{2\beta(1 - \beta + \beta^2)} - \frac{3 \log \rho_1}{(2 - \beta)^2} \right] - \frac{3}{\rho_1(2 - \beta)} + n \left[\frac{3\beta\beta'}{2(2 - \beta)(1 - \beta + \beta^2)} + \frac{1}{\rho_1 \log \rho_1} \right] \right\} \quad (29)$$

in which

$$\beta' = \frac{\rho_1 - \rho_e \beta}{l^2 + \rho_1 \rho_e - \rho_e^2} \quad (30)$$

The instability condition

$$d\alpha/d\rho_1 = 0$$

will be satisfied if either f_1' or $d\alpha/d\rho_e = 0$. Now $d\alpha/d\rho_e$ will always be positive, since $d\alpha/d\rho_e = 0$ corresponds to the burst pressure in the limiting case $l = 0$. Figures 2 and 3 show that burst pressures are maximum for this case; hence the instability condition reduces to

$$f_1' = 0 \quad (31)$$

The values of the various parameters at burst can be determined for given values of l and n by satisfying Eqs. (21, 22, and 31) simultaneously. For the case $n = 0$, the pressure-displacement relation is given by Eq. (24). Differentiating, the instability condition is found to be

$$\frac{d\alpha}{d\rho_1} = \alpha \left\{ \beta \left[\frac{2 - \beta}{2\beta(1 - \beta + \beta^2)} - \frac{3 \log \rho_1}{(2 - \beta)^2} \right] - \frac{3}{\rho_1(2 - \beta)} \right\} = 0 \quad (32)$$

where now

$$\beta' = (\rho_1 - \beta)/(l^2 + \rho_1 - 1) \quad (33)$$

and where β is given by Eq. (23). Values of α at burst can be found for a given value l by satisfying Eqs. (24) and (32) simultaneously. However, as Fig. 2 shows, $d\alpha/d\rho_1$ is always negative for sufficiently long shells. These shells are initially unstable. The instability pressure found by substituting values of $\rho_1 = 1$ and $\beta = \frac{1}{2}$ into Eq. (24) is $\alpha^* = 2/3^{1/2}$. The critical length is determined by using these values of ρ_1 and β in Eqs. (31) and (32). In this way, it is found that for stable shells $l \leq 1/2^{1/2}$.

Curves of instability pressure vs n are shown in Fig. 4 for values of $l = 0.5, 1.0, 2.0$, and 3.0 . Corresponding curves

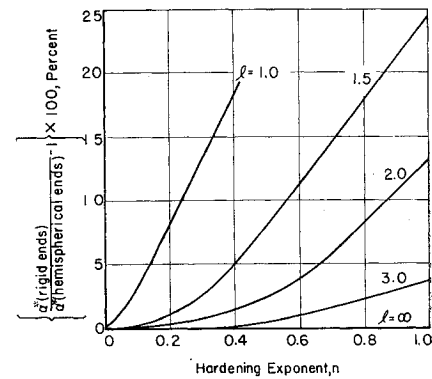


Fig. 5 Excess strength of rigidly capped cylinder over hemispherically capped cylinder.

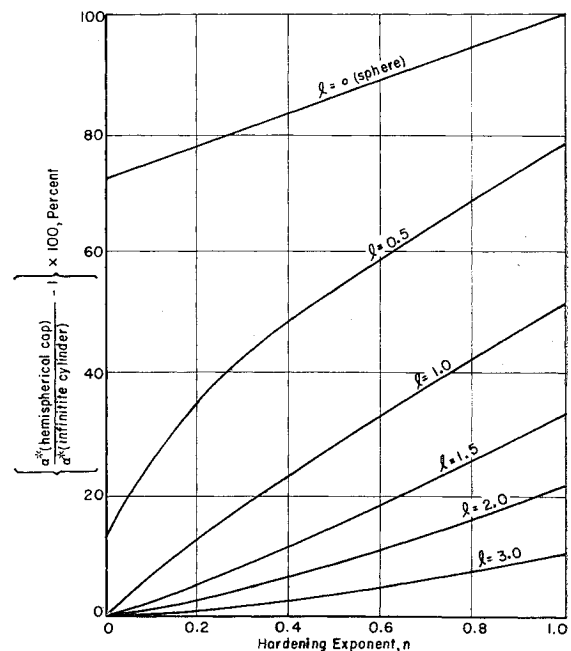


Fig. 6 Excess strength of hemispherically capped finite cylinder over infinite cylinder.

also are given for the sphere and infinite cylinder. Comparisons of the burst strength of cylinders with hemispherical heads with that of cylinders with rigid ends⁵ and infinite cylinders are made in Figs. 5 and 6, respectively.

V. Conclusions

The results indicate that the strength of cylinders of finite length with hemispherical heads is greater than that of the infinite cylinders for the range of strains up to burst. This excess strength increases with increasing strain, with increasing values of the hardening exponent, and with decreasing values of length-diameter ratio. The effects of end restraint appear to be negligible for length-diameter ratios greater than about two for the range of values of the hardening exponent of greatest practical interest ($n \leq 0.3$).

Table 1 Stress-strain properties in simple tension

Material	Strength coefficient σ_0 , psi	Hardening exponent n	Yield stress, psi
A212 grade B firebox steel	155,000	0.245	32,000
A295 grade C firebox steel	117,000	0.278	27,5000
T-304 stainless steel	193,000	0.959	40,400
A302 steel	133,000	0.197	52,190
USS T-1 steel	178,700	0.087	119,800
0.15% carbon steel	108,000	0.285	32,700

Values of the strength coefficient σ_0 and the hardening exponent n for a number of steels are given in Table 1. These data are taken from an extensive list compiled by Marin.⁸ Descriptions of methods for obtaining the values of σ_0 and n from tensile test data are given in Refs. 7 and 9. With the exception of type-304 stainless, a highly ductile austenitic steel, the values of n given in Table 1 lie in the range $0 \leq n \leq 0.3$. It can be shown⁹ that the strain at maximum load in a tensile test is equal to n for a material with a stress-strain relation of the form $\sigma = \sigma_0 \epsilon^n$. Hence, high-strength steels, since they have little ductility, have the smallest values of n .

References

¹ Salmon, M. A., "Plastic instability of cylindrical shells with rigid end closures," Am. Soc. Mech. Engrs. 63-APM-13 (June 24, 1963).

² Weil, N. A. and Newmark, N. M., "Large plastic deformations of circular membranes," J. Appl. Mech. 4, 533-538 (1955).

³ Grigoriev, A. S., "State of stress in cylindrical membrane shells at large deformations," Prikl. Math. Mech. 21, 827-832 (1957).

⁴ Grigoriev, A. S., "Equilibrium of a membrane of revolution at large deformations," Prikl. Math. Mech. 25, 1083-1090 (1961).

⁵ Weil, N. A., "An approximate solution for the bursting of thin-walled cylinders," Intern. J. Mech. Sci. (to be published).

⁶ Hill, R., *The Mathematical Theory of Plasticity* (Oxford University Press, London, 1956), Chap. II.

⁷ Svenson, N. L., "The bursting pressure of cylindrical and spherical vessels," J. Appl. Mech. 25, 89-96 (1958).

⁸ Marin, J. and Weng, T., "Strength of thick walled cylindrical pressure vessels," Dept. Eng. Mech., Pennsylvania State Univ. (1961).

⁹ Marin, J., *Mechanical Behavior of Engineering Materials* (Prentice Hall Inc., Englewood Cliffs, N. J., 1962), Chap. 1.

SEPTEMBER 1963

AIAA JOURNAL

VOL. 1, NO. 9

Bending Vibrations of a Circular Cylindrical Shell with an Internal Liquid Having a Free Surface

ULRIC S. LINDHOLM,* WEN-HWA CHU,* DANIEL D. KANA,† AND H. NORMAN ABRAMSON‡
Southwest Research Institute, San Antonio, Texas

Resonant bending frequencies and mode shapes were determined experimentally for a thin circular cylindrical shell containing an internal liquid with a free surface. The measured increase in frequency between uncapped and capped partially filled tanks of two different end conditions are generally in agreement with theoretical predictions. Differences between theory and experiment are attributed primarily to variations of actual mode shapes from those assumed in the theory. This is true for both cantilever and pin-ended tanks, with the latter being even more complicated by a strong dependence of mode shape on liquid depth. Significant coupling occurred between bending and breathing shell responses, becoming increasingly important with decreasing tank-fineness ratio.

Introduction

THIS paper represents a continuation of the authors' studies of the dynamic interaction of a flexible tank with an internally contained liquid. A previous paper¹ dealt with the effect of the internal liquid column on the *breathing* vibrations of the tank wall. The present study is concerned with the coupled tank-liquid system resonant *bending* frequency for thin circular cylindrical shells and, particularly, with the effect of the liquid free surface motion on the coupled bending resonance. The studies were initiated using uniform shells, where the coupled resonant frequencies were at least an order of magnitude greater than the uncoupled liquid free surface resonances. In subsequent work a theoretical investigation was made of the behavior of tanks with added tip masses, in order to establish the influence of coupling when the bending resonance is in the neighborhood of the lower sloshing resonances. This latter condition more nearly approximates the condition in actual launch vehicles.

Presented at the IAS 31st Annual Meeting, New York, January 21-23, 1963; revision received July 8, 1963. The results reported in this paper were obtained during the course of research sponsored by NASA under Contract NASw-146. The authors are indebted to the Southwest Research Institute's Computations Laboratory for performing the theoretical calculations and to Gilbert F. Rivera for preparing the illustrations.

* Senior Research Engineer, Department of Mechanical Sciences.

† Research Engineer, Department of Mechanical Sciences.

‡ Director, Department of Mechanical Sciences. Associate Fellow Member AIAA.

Available theoretical analyses show that the presence of the liquid free surface, with its associated sloshing modes, may shift the fundamental bending frequency of the liquid-flexible tank system by an appreciable amount over that which would occur if the free surface motion were not present. Problems of flexible tank dynamics are therefore important from the point of view of the missile designer, who must have precise knowledge of the system resonant frequencies in order that unduly large structural stresses are not created and also that the structural resonances do not occur in the neighborhood of the missile control system frequencies and thus produce serious coupling effects. The present program was initiated in order to verify experimentally the existing analyses of the free bending vibrations of a tank, partially filled with a liquid.

Miles² has derived the frequency equation for the liquid-filled circular cylindrical tank including free liquid surface effects using the Lagrangian energy approach. Particular results cited by Miles in his paper give increases in the fundamental resonant bending frequency resulting from liquid sloshing of 5% and 27% for full cantilever and freely supported tanks of fineness ratio equal to one. This indicates that in order to determine resonant frequencies accurately it is necessary to take into account the free surface boundary condition in determining the total apparent mass of the liquid. The free surface coupling always results in an *increase* in the resonant bending frequency over that for the capped tank.[§]

§ Here, and throughout this paper, a capped tank refers to one in which the liquid sloshing motion is suppressed, i.e., the free surface remains a plane surface normal to the tank generator.